



**HAL**  
open science

## A CBS domain-containing pyrophosphatase of *Moorella thermoacetica* is regulated by adenine nucleotides

Joonas Jämsen, Heidi Tuomunen, Anu Salminen, Georgiy A. Belogurov,  
Natalia N. Magretova, Alexander A. Baykov, Reijo Lahti

### ► To cite this version:

Joonas Jämsen, Heidi Tuomunen, Anu Salminen, Georgiy A. Belogurov, Natalia N. Magretova, et al.. A CBS domain-containing pyrophosphatase of *Moorella thermoacetica* is regulated by adenine nucleotides. *Biochemical Journal*, 2007, 408 (3), pp.327-333. 10.1042/BJ20071017 . hal-00478856

**HAL Id: hal-00478856**

**<https://hal.science/hal-00478856>**

Submitted on 30 Apr 2010

**HAL** is a multi-disciplinary open access archive for the deposit and dissemination of scientific research documents, whether they are published or not. The documents may come from teaching and research institutions in France or abroad, or from public or private research centers.

L'archive ouverte pluridisciplinaire **HAL**, est destinée au dépôt et à la diffusion de documents scientifiques de niveau recherche, publiés ou non, émanant des établissements d'enseignement et de recherche français ou étrangers, des laboratoires publics ou privés.

## A CBS domain-containing pyrophosphatase of *Moorella thermoacetica* is regulated by adenine nucleotides

Joonas JÄMSEN<sup>\*1</sup>, Heidi TUOMINEN<sup>\*1</sup>, Anu SALMINEN<sup>\*</sup>, Georgiy A. BELOGUROV<sup>\*</sup>, Natalia N. MAGRETOVA<sup>†</sup>, Alexander A. BAYKOV<sup>†</sup> and Reijo LAHTI<sup>\*2</sup>

<sup>\*</sup>Department of Biochemistry and Food Chemistry, University of Turku, FIN-20014 Turku, Finland, and <sup>†</sup>A. N. Belozersky Institute of Physico-Chemical Biology, Moscow State University, Moscow 119899, Russia

Short title: Nucleotide-regulated CBS-pyrophosphatase

Abbreviations used: CBS, cystathionine- $\beta$ -synthase; DTPA, diethylenetriaminepentaacetic acid; PPase, inorganic pyrophosphatase; *mt*CBS-PPase, CBS domain-containing PPase from *Moorella thermoacetica*.

<sup>1</sup> These two authors contributed equally to this work.

<sup>2</sup> To whom correspondence should be addressed [email reijo.lahti@utu.fi (R. L.) or baykov@genebee.msu.su (A. A. B.)].

All prepublication correspondence should be addressed to:

Reijo Lahti  
Professor of Biochemistry  
Department of Biochemistry  
University of Turku  
FIN-20014 Turku, Finland  
Tel: 358 2 333-6845  
Fax: 358 2 333-6860  
E-mail: reijo.lahti@utu.fi

Cystathionine- $\beta$ -synthase (CBS) domains are found in proteins from all kingdoms of life, and point mutations in these domains are responsible for a variety of hereditary diseases in humans; however, the functions of CBS domains are not well understood. Here, we cloned, expressed in *Escherichia coli*, and characterized a family II inorganic pyrophosphatase (PPase) from *Moorella thermoacetica* (*mtCBS*-PPase) that has a pair of tandem 60-amino acid CBS domains within its N-terminal domain. Because *mtCBS*-PPase is a dimer and requires transition metal ions ( $\text{Co}^{2+}$  or  $\text{Mn}^{2+}$ ) for activity, it resembles common family II PPases, which lack CBS domains. The *mtCBS*-PPase, however, has lower activity than common family II PPases, is potently inhibited by ADP and AMP, and is activated up to 1.6-fold by ATP. Inhibition by AMP is competitive whereas inhibition by ADP and activation by ATP are both of mixed types. The nucleotides are effective at nanomolar (ADP) or micromolar concentrations (AMP and ATP) and appear to compete for the same site on the enzyme. The nucleotide binding affinities are thus 100- to 10,000-fold higher than for other CBS domain-containing proteins. Interestingly, genes encoding CBS-PPase occur most frequently in bacteria that have a membrane-bound  $\text{H}^+$ -translocating PPase with a comparable  $\text{PP}_i$ -hydrolyzing activity. Our results suggest that soluble nucleotide-regulated PPases act as amplifiers of metabolism in *M. thermoacetica* by enhancing or suppressing ATP production and biosynthetic reactions at high and low  $[\text{ATP}]/([\text{AMP}] + [\text{ADP}])$  ratios, respectively.

Key words: inorganic pyrophosphatase, CBS domain, *Moorella thermoacetica*, bidirectional regulation, phylogenetic analysis, quaternary structure.

## INTRODUCTION

Inorganic pyrophosphate (PP<sub>i</sub>) is produced in vast amounts by biosynthetic reactions, such as protein, RNA, and DNA synthesis, and its concentration affects the equilibria of these reactions [1]. In addition, PP<sub>i</sub> regulates many other cellular processes, including calcification, cell proliferation, and iron transport [2]. Consequently, disruption of PP<sub>i</sub> metabolism can lead to a variety of pathological conditions [2].

PP<sub>i</sub> is mainly hydrolyzed to orthophosphate by inorganic pyrophosphatase (PPase) (EC 3.6.1.1), an enzyme that is essential for life [3–6]. There are two known types of PPase: soluble and integral membrane-bound. Soluble PPases are further subdivided into families I and II, which are not homologous [7,8]. Family I PPases are found in all kingdoms of life and are among the best-characterized phosphoryl transfer enzymes [9,10]. Family II PPases, which were discovered more recently [7,8], are found in *Bacilli* and *Clostridia* and in some other bacterial lineages, including several human pathogens, and belong to the DHH family of phosphohydrolases [11]. Family II PPases are homodimers of subunits formed by two well-defined domains, whereas family I PPases have two or six compact one-domain subunits. The N- and C-terminal domains of family II PPases are connected by a flexible linker, and the active site is located at the domain interface [12,13]. Also, unlike family I PPases, family II PPases contain a tightly bound transition metal ion, usually Mn<sup>2+</sup> or Co<sup>2+</sup>, although they also require Mg<sup>2+</sup> for maximal activity. In addition, divalent cations, especially Mn<sup>2+</sup>, promote dimerization of family II PPases [14].

Interestingly, the N-terminal domain of approximately a quarter of the known family II PPase sequences contains a large (~250-amino acid) insert, comprising two CBS domains. None of these CBS-PPases has been isolated and characterized. CBS domains, originally found in cystathionine-β-synthase [15], are widely distributed among proteins in all three kingdoms of life, but their roles are not well understood [16,17]. In some cases, CBS domains are potential targets for regulation by adenosine derivatives [16–21]. Importantly, point mutations in CBS domains cause several hereditary diseases in humans [17].

To elucidate the role of CBS domains in family II PPases, we cloned, expressed, and purified a CBS-PPase from *Moorella thermoacetica* (former name *Clostridium thermoaceticum*), a low G + C Gram-positive thermophilic acetogen with an optimum growth temperature at 55–60°C [22]. We found that, unlike all other known PPases, this enzyme is subject to a strong bidirectional regulation by adenine nucleotides.

## EXPERIMENTAL

### Cloning and mutagenesis

Genomic DNA extracted from *M. thermoacetica* strain ATCC 35608 was obtained from Deutsche Sammlung von Mikroorganismen und Zellkulturen GmbH (DSMZ). The *mtCBS*-PPase open reading frame (GenBank accession number NC\_007644) was amplified by PCR using primers 5'-TTATCATATGGGTAAAGAGAT TCTGGTTATCG-3' (forward) and 5'-TTATC TCGAGTTATCCCTGCAGCAACCGCCG-3' (reverse). The amplified gene was sequenced in both directions and one difference compared to the sequence shown in GenBank was observed (TTG encoding Leu190 was replaced by CTG), but this did not affect the protein sequence. The PCR fragment was inserted into pBLUESCRIPT SK (Stratagene) and site-directed mutagenesis was performed using an overlapping PCR technique (QuikChange, Stratagene). The mutation was verified by DNA sequencing.

### Protein expression and purification

To produce wild-type and variant *mtCBS*-PPases, the PCR products were cloned into the pET36b vector (Novagen) using *Nde*I and *Xho*I. The plasmid construct was transformed into *Escherichia coli* BL21(DE3) RIL cells (Stratagene) and the transformants were grown in Terrific Broth [23] containing 30 µg/mL kanamycin and 30 µg/mL chloramphenicol. *mtCBS*-PPase expression was induced for 3 h by 0.4 mM isopropyl-β-D-thiogalactopyranoside.

Cell paste (10 g wet weight) obtained by centrifugation was resuspended in 30 ml of ice-cold 25 mM Tris-HCl buffer, pH 7.3, containing 24 mM MgCl<sub>2</sub>, 1 mM CoCl<sub>2</sub>, 20 µM diethylenetriaminetetraacetic acid (DTPA) and homogenized twice with a French press (SLM Instruments) at 900 psi. The crude extract obtained was loaded onto a 150-ml column containing Fast Flow DEAE-Sepharose (GE Healthcare). The column was washed with the same buffer, and protein was eluted with a 450-ml linear gradient of 0.1–0.3 M NaCl. Fractions containing *mtCBS*-PPase (150–190 mM NaCl) were pooled, concentrated to 12 ml with Centriprep10 (Amicon), and further purified by gel filtration on a Superdex 200 26/60 column (GE Healthcare) equilibrated with 50 mM Tris-HCl buffer, pH 7.5, containing 50 mM KCl, 2 mM MgCl<sub>2</sub>, 0.1 mM CoCl<sub>2</sub> and 20 µM DTPA. The fractions containing *mtCBS*-PPase were pooled, concentrated to 20–40 mg/mL and stored frozen at –70°C.

Because the enzyme was most stable in the presence of 0.1 mM Co<sup>2+</sup> and 2 mM Mg<sup>2+</sup>, these cations were routinely added to the solutions used to purify, store, and dilute the enzyme. When needed, these metal ions were removed from the enzyme stocks by incubation

with 5 mM DTPA for 1 day at 4°C. The bulk of the chelator was removed by dialysis against three 1-l changes of 100 mM Mops-KOH buffer (pH 7.5) containing 50  $\mu$ M DTPA.

The purity of enzyme samples was assessed by electrophoresis on 8–25% gradient polyacrylamide gels in the presence of 0.55% sodium dodecyl sulfate using the Phast System (GE Healthcare). Concentrations of *mt*CBS-PPase solutions were determined on the basis of a subunit molecular mass of 48.1 kDa and an extinction coefficient  $\epsilon^{1\%}_{280}$  of 4.5, as estimated from the amino acid composition using the ProtParam program [24].

### Activity measurements

Except where noted, the activity was measured at 25°C in 25 ml of 100 mM Mops-KOH buffer (pH 7.2) containing 0.1 mM CoCl<sub>2</sub>, 5 mM MgCl<sub>2</sub>, and the nucleotide tested. An aliquot (5–150  $\mu$ l) of diluted enzyme solution was added to the mixture (0.2–2  $\mu$ g/mL final enzyme concentration), followed 1 min later by 0.16 mM PP<sub>i</sub>. The formation of P<sub>i</sub> was then monitored for 3–10 min using an automatic P<sub>i</sub> analyzer [25], and initial reaction rates were estimated from the recorder tracing.

AMP, ADP, and ATP were from Fluka. All other nucleotides were from Sigma. AMP was the free acid, ADP was the potassium salt, and all other nucleotides were sodium salts. Immediately prior to the use of ATP, any contaminating ADP was converted to ATP by treating 5 mM stock solutions of ATP for 1 h at room temperature with 10 U/mL rabbit muscle creatine kinase (Roche) in 100 mM Mops-KOH buffer (pH 7.2) containing 10 mM creatine phosphate (Fluka) and 5 mM MgCl<sub>2</sub>. The AMP preparation was judged to be reasonably pure because a similar treatment with creatine kinase and creatine phosphate had no effect on the PPase activity measured in the presence of AMP. In addition, treating stock ADP solutions with 10 U/mL of hexokinase and 10 mM glucose to convert any contaminating ATP into ADP also had no effect on the PPase activity. For competition measurements, in which ADP and ATP were added simultaneously, creatine kinase in stock solutions of ATP was removed by ultrafiltration using Vivaspin 4 ml concentrators (Sartorius AG) with a 10 kDa MWCO PES membrane.

### Sedimentation

Analytical ultracentrifugation was carried out at 20°C in a Spinco E instrument (Beckman Instruments) with scanning at 280 nm. The samples contained 10  $\mu$ M enzyme and appropriate ligands. Before each run, the samples were incubated for 2 to 3 h at 20°C. The sedimentation velocity was measured at 48,000 rpm, and the sedimentation coefficient ( $s_{20,w}$ ) was calculated as described by Chervenka [26].

### Crosslinking and electrophoresis

Enzyme was diluted to 8.3  $\mu\text{M}$  with 25 mM HEPES-KOH (pH 7.5) and then incubated with 26 mM glutaraldehyde for 15 or 30 min at room temperature [27]. The reaction was stopped by addition of 1/10 volume of 1.0 M Tris-HCl (pH 7.3). The samples were separated by electrophoresis on Phast System 8–25% SDS-PAGE gradient gels (GE Healthcare), and the gels were stained with PhastGel Blue R (GE Healthcare). A Perfect Protein Marker kit (Novagen) was used as molecular weight standards.

### Kinetic data analysis

Nonlinear least squares fitting of the data was performed using SCIENTIST, version 2.01 (Micromath). The dependence of activity on the concentration of the ligand (L) was fit to eqn 1, where  $A_{+L}$  and  $A_{-L}$  are activities with and without bound ligand, respectively, and  $K_d$  is the apparent dissociation constant of the enzyme-ligand complex, all measured at a fixed substrate concentration:

$$A = A_{+L} + (A_{-L} - A_{+L}) / (1 + [L]/K_d) \quad (1)$$

In competition experiments, the dependence of the apparent  $K_d$  ( $K_{d,app}$ ) for ligand  $L_1$  on the concentration of the second ligand,  $L_2$ , was fit to eqn 2, where  $K_{d1}$  and  $K_{d2}$  are the dissociation constants for ligands  $L_1$  and  $L_2$ , respectively:

$$K_{d,app} = K_{d1} (1 + [L_2]/K_{d2}) \quad (2)$$

## RESULTS

### Expression, purification and catalytic activity of mtCBS-PPase

SDS-PAGE analysis of crude extracts obtained from recombinant *E. coli* cells revealed an intense ~50 kDa band that was absent in cells transformed with empty pET36b vector (data not shown). The SDS-PAGE also indicated that mtCBS-PPase represented ~10% of the total protein. The recombinant protein was easily purified to homogeneity by ion exchange chromatography and gel filtration. This procedure yielded 30–40 mg of pure mtCBS-PPase per liter of cell culture (~6 g of cell paste). *E. coli* PPase, which belongs to family I of soluble PPases, was absent from the purified mtCBS-PPase because the former eluted at a 20 mM lower NaCl concentration during DEAE-Sepharose chromatography.

The purified mtCBS-PPase exhibited a maximal  $k_{cat}$  value ( $1.7 \text{ s}^{-1}$ ) when assayed in the presence of both 1 mM  $\text{Mg}^{2+}$  and 0.1 mM  $\text{Co}^{2+}$ . Replacement of  $\text{Co}^{2+}$  by  $\text{Mn}^{2+}$  reduced  $k_{cat}$  to  $0.65 \text{ s}^{-1}$ . The  $k_{cat}$  values observed in the presence of  $\text{Co}^{2+}$ ,  $\text{Mn}^{2+}$  or  $\text{Mg}^{2+}$  alone were 1.15, 0.36 and  $0.01 \text{ s}^{-1}$ , respectively. According to its cofactor specificity, mtCBS-PPase resembles the

common-type family II PPase of *Methanococcus jannaschii* [28]. However, the maximal observed  $k_{\text{cat}}$  value for *mtCBS*-PPase at 25°C was three orders of magnitude lower than that for common family II PPases [14] and was only two-fold higher at 55°C, the growth temperature of *M. thermoacetica*.

### Effects of nucleotides and nucleosides

Table 1 shows that *mtCBS*-PPase is strongly inhibited by 100  $\mu\text{M}$  AMP and ADP, whereas ATP activates it 1.6-fold. Some nucleotides, including cAMP, CDP, and UDP were less effective at inhibiting *mtCBS*-PPase, and most other nucleotides and nucleosides did not significantly affect the activity. Thus, adenine nucleotides are effective modulators of *mtCBS*-PPase activity. This is strikingly different than the common type family II PPase from *Bacillus subtilis* and family I PPases from *E. coli* and other sources, which are not modulated by ATP, ADP, or AMP and lack CBS domains.

### Kinetic analysis of adenine nucleotide effects

Figure 1 shows the dose dependencies of AMP, ADP and ATP effects measured at a fixed substrate concentration (160  $\mu\text{M}$  total  $\text{PP}_i$ ). Each curve obeyed Eq. 1 for activation or nonlinear inhibition with a finite activity of the enzyme-inhibitor complex. The relative values of these activities ( $A_{+L}/A_{-L}$ ) for AMP and ADP were low but significantly different from zero (Table 2). The apparent binding constants ( $K_d$ ) derived for each nucleotide from these profiles are also summarized in Table 2. As expected from the appearance of the profiles in Figure 1, the  $K_d$  values were similar for AMP and ATP and an order of magnitude lower for ADP.

The nucleotide effects on activity were further analyzed using a Lineweaver-Burk plot. Surprisingly, the inhibition by AMP and ADP was of different types. AMP increased only the Michaelis constant (Figure 2, *top*) and was thus a competitive inhibitor, whereas ADP additionally decreased the maximal velocity (Figure 2, *bottom*) and was thus a mixed-type inhibitor. The effect of ATP on the kinetic parameters was the opposite of that of ADP (Figure 2, *top*). At 10  $\mu\text{M}$ , ATP decreased the Michaelis constant (from  $10.6 \pm 0.5 \mu\text{M}$  to  $7.0 \pm 0.6 \mu\text{M}$ ) and increased the maximal velocity (from  $1.69 \pm 0.05 \text{ s}^{-1}$  to  $2.3 \pm 3 \text{ s}^{-1}$ ). True inhibition constants governing AMP binding to substrate-free enzyme ( $K_i = 19 \pm 2 \text{ nM}$ ) and ADP binding to substrate-free enzyme ( $K_i = 1.3 \pm 0.1 \text{ nM}$ ), and to the enzyme-substrate complex ( $K_i' = 0.35 \pm 0.03 \mu\text{M}$ ) were estimated from the secondary dependencies shown in the insets of Figure 2. The substrate thus afforded partial protection against inhibition by ADP and completely prevented inhibition by AMP. The residual activity of the nucleotide-bound enzyme was ignored in this analysis as this activity would have only a minor effect on



estimated parameter values. For ATP, true binding constants governing binding to substrate-free enzyme ( $K_a$ ) and to enzyme-substrate complex ( $K_a'$ ) were not determined separately, but their ratio,  $K_a'/K_a$ , should be close to the ratio of the Michaelis constants measured at ATP concentrations of zero and near-saturating (10  $\mu\text{M}$ ), *i.e.*,  $1.5 \pm 0.2$ . That  $K_a'/K_a$  exceeds unity is also evidenced by the fact that the lines measured in the absence and in the presence of ATP intersected above the ordinate axis in Figure 2, *top*.

To investigate interactions of inhibiting and activating nucleotides on *mtCBS-PPase* activity, the profiles of ADP modulation were measured at several fixed ATP concentrations and *vice versa* (Figure 3). ATP protected *mtCBS-PPase* from inhibition by ADP by decreasing the sensitivity to ADP (*i.e.*, by shifting the dose-response inhibition curve to the right) and by increasing the basal activity in the absence of ADP. The  $K_{d,app}$  for ADP changed in proportion to the ATP concentration (Figure 3, *top inset*) up to 100  $\mu\text{M}$  ATP, which is 500 times the  $K_d$  for ATP. Similarly, the  $K_{d,app}$  for ATP was a linear function of the ADP concentration up to 0.2  $\mu\text{M}$  ADP (Figure 3, *bottom inset*), which is 80 times the  $K_d$  for ADP. These results indicated that the binding of ADP and ATP was mutually exclusive in the concentration ranges tested. If a mixed  $\text{E}\cdot\text{ADP}\cdot\text{ATP}$  and/or  $\text{E}\cdot\text{S}\cdot\text{ADP}\cdot\text{ATP}$  complex were formed,  $K_{d,app}$  for ADP would have attained a constant level, intermediate between the  $K_d$  values for ADP binding to  $\text{E}\cdot\text{ATP}$  and  $\text{E}\cdot\text{S}\cdot\text{ATP}$ . These considerations also apply to the bottom panel of Figure 3. Qualitatively similar inhibition/activation patterns were observed for the pair AMP/ATP (data not shown). The effective concentrations of AMP were, however, higher than those of ADP by an order of magnitude. The binding constants derived for each nucleotide, from data in the insets to Figure 3, are summarized in Table 2.

The effects of the adenine nucleotides on  $\text{Mn}^{2+}/\text{Mg}^{2+}$ -activated *mtCBS-PPase* were qualitatively similar to those observed for the  $\text{Co}^{2+}/\text{Mg}^{2+}$ -activated form (Figure 1). The  $K_d$  values for AMP and ADP were also similar, but the  $K_d$  value for ATP was 10-fold higher (Table 2). Furthermore, the relative residual activities at infinite AMP or ADP concentrations ( $A_{+L}/A_{-L}$ ) were markedly higher in the presence of  $\text{Mn}^{2+}$ . Finally, AMP, ADP, and ATP had similar effects on  $\text{Co}^{2+}/\text{Mg}^{2+}$ -activated *mtCBS-PPase* at 55°C, which is the physiological temperature for *M. thermoacetica* (data not shown).

### Effect of Y169A substitution on adenine nucleotide binding

Tyr-169 is located in the CBS domain of *mtCBS-PPase*, in the region corresponding to the nucleotide binding pocket of the chloride transporter ClC-5, another CBS domain protein whose three-dimensional structure has been recently determined [29]. Consistent with this localization, the replacement of Tyr-169 with Ala markedly decreased the affinity of *mtCBS-*

PPase for the adenine nucleotides (Table 2), while having only a small effect (1.8-fold activation) on enzyme hydrolytic activity measured in their absence. Qualitatively, the Y169A variant behaved similarly to wild type *mtCBS*-PPase and exhibited activation by ATP and inhibition by AMP and ADP (Table 2).

### Quaternary structure of *mtCBS*-PPase

Common family II PPases are dimeric proteins in the presence of metal cofactors but dissociate into nearly inactive monomers in the absence of such cofactors [14,30]. As CBS domains are reported to control oligomerization of cystathionine- $\beta$ -synthase [31,32], we determined the oligomeric structure of *mtCBS*-PPase in the absence and presence of adenine nucleotides and compared it with that of common family II PPases. The sedimentation coefficient ( $s_{20,w}$ ) at pH 7.2 was  $6.4 \pm 0.1$  S for the metal-depleted *mtCBS*-PPase and increased to  $7.7 \pm 0.1$ ,  $7.9 \pm 0.2$ , and  $7.6 \pm 0.1$  S in the presence of 100  $\mu$ M  $\text{CoCl}_2$ , 100  $\mu$ M  $\text{MnCl}_2$ , and 1 mM  $\text{MgCl}_2$ , respectively. Adenine nucleotides (AMP, ADP, and ATP) at 100  $\mu$ M had no effect on the  $s_{20,w}$  value for *mtCBS*-PPase measured in the presence of 100  $\mu$ M  $\text{CoCl}_2$ .

The values of  $s_{20,w}$  for *mtCBS*-PPase measured in the presence of the metal ions were somewhat higher than that predicted assuming a spherical protein with a molecular weight of 96 kDa (dimer of 48 kDa monomers). Therefore, we performed crosslinking experiments to confirm that this enzyme is a dimer. Specifically, we reacted *mtCBS*-PPase with glutaraldehyde and separated the products by SDS-PAGE. Almost all of the protein migrated as the crosslinked dimer, although a small amount of unreacted monomer was observed (Figure 4). Similar electrophoresis patterns were obtained for *mtCBS*-PPase treated with glutaraldehyde in the presence of different metal ions or at various concentrations of *mtCBS*-PPase. The relative amount of the monomer, however, slightly increased in the absence of the metal ions or at low enzyme concentrations. Collectively, our data indicate that the oligomeric structure of *mtCBS*-PPase is similar to that of common family II PPases, which lack CBS domains, and is not affected by nucleotide binding.

### DISCUSSION

CBS domains are found both in cytosolic enzymes and membrane-associated enzymes and channels from all species. They usually occur as tandem repeats, which are independent units that retain their structure and binding properties even when separated from the bulk protein [17]. The importance of CBS domains is emphasized by the observations that mutations of

their conserved residues impair AMP, ATP, and *S*-adenosyl methionine binding to the CBS domains and cause a variety of human hereditary diseases [16,17]. Although they are thought to be regulatory domains, the experimental evidence for this is scarce. Because CBS domains bind adenine nucleotides with varying affinities, they may act as sensors of cellular energy status [16,17]. More recently, CBS domains of the chloride channel CLC-5 have been implicated in the control of intracellular trafficking [33] and the gating of the osmoregulatory transporter OpuA by osmotic strength [34].

### **CBS domains as regulators of *mt*CBS-PPase**

Several lines of evidence suggest that the modulation of *mt*CBS-PPase by nucleotides is also mediated by CBS domains. First, isolated CBS domains from several proteins can bind adenine nucleotides [16,17,20], whereas common family II PPases that lack CBS domains do not bind adenine nucleotides [35]. Second, a single Y169A replacement in the CBS domain suppressed nucleotide binding to *mt*CBS-PPase, but increased enzyme catalytic activity. Finally, the mixed type inhibition of *mt*CBS-PPase by ADP, and the activation by ATP, indicate formation of a ternary enzyme-substrate-nucleotide complex and are therefore inconsistent with nucleotide binding at the active site.

The observed competition between ATP binding, and the binding of both AMP and ADP, as well as the structural similarities between these compounds, imply a common binding site for all nucleotides on *mt*CBS-PPase. This conclusion is supported by structural data reported for other proteins. To date, a high-resolution three-dimensional structure is available for only a single intact CBS domain-containing protein, namely IMP dehydrogenase, but it does not contain bound nucleotides in the CBS domain [36]. However, three-dimensional structures have been determined for several truncated CBS domain-containing proteins [29,37,38]. The most recent structures of the cytoplasmic part of the chloride transporter CLC-5 [29] contain bound ADP or ATP, and those of the C-terminal domain of AMP-activated protein kinase (Protein Data Bank entries 2O0X and 2O0Y) contain bound AMP or ATP, at the same site, formed between two CBS domains. Importantly, the new structures suggest that the nucleotides cause a marked conformational change in the CBS domains, thus explaining nucleotide regulatory action.

Although all polar active site residues found in common family II PPases [12,13] are conserved in *mt*CBS-PPase, even in the presence of the best metal cofactor,  $\text{Co}^{2+}$ , *mt*CBS-PPase is less active than common family II PPases by three orders of magnitude. Therefore, the insert containing two CBS domains appears to severely disrupt the normal catalytic cycle. Importantly, such an “internally inhibited” system should be very sensitive to structural

changes caused by nucleotide binding to the CBS domains and could easily be inhibited or activated. In this context, ATP partially compensates for the effect of the CBS insertion, whereas AMP and ADP increase the effect.

### **Nucleotide specificity of mtCBS-PPase**

Nucleotide binding to *mtCBS-PPase* was highly specific with respect to both the base and the phosphate moieties. At a concentration of 100  $\mu\text{M}$ , adenine nucleotides were the most potent regulators of the enzyme. When guanine and uridine nucleotides were examined, only the diphosphates had significant effects on the activity of *mtCBS-PPase*; this may be because these nucleotides bound with weaker affinities.

The phosphate moiety of the nucleotide is also important, and determines both binding affinity (adenosine does not bind), and whether the nucleotide acts as an activator or inhibitor. A diphosphate seems to result in the highest binding affinity, but a triphosphate is needed for activation. Moreover, the phosphate moiety determines the relative affinities of the nucleotide for free enzyme and enzyme-substrate complex. AMP, ADP and ATP can all combine with substrate-free enzyme whereas only ADP and ATP can bind, though with lower affinity, to the enzyme-substrate complex. Accordingly, the inhibition type is competitive with AMP and mixed with ADP, and ATP is a mixed-type activator. Substrate thus interferes with adenine nucleotide binding and *vice versa*, and the effect decreases with increases in phosphate chain length, especially when comparing AMP effects with ADP effects. A likely structural explanation of these data is that both the  $\alpha$ -phosphate and the  $\beta$ -phosphate are involved in strong, thermodynamically favorable, interactions, that stabilize inactive conformations of *mtCBS-PPase*, whereas the interaction with the  $\gamma$ -phosphate is thermodynamically unfavorable but gives rise to an active enzyme conformation. The conformations elicited by AMP and ADP are different because their complexes bind substrate differently. Although a direct contact of the nucleotide phosphate chain with the active site cannot presently be excluded, it seems unlikely, because ATP, which has the longest phosphate chain, facilitated substrate binding by lowering  $K_m$  (Figure 2). The assumed conformational flexibility of *mtCBS-PPase* is consistent with the known structures of common family II PPases, in which active sites lie between two domains connected by a highly flexible linker [12,13]. The dependence of the nucleotide effect on the length of the phosphate moiety may be due, but only in part, to  $\text{Mg}^{2+}$  binding; in the presence of 5 mM  $\text{Mg}^{2+}$ , ATP and ADP predominantly exist as complexes with  $\text{Mg}^{2+}$ , whereas AMP exists as a mixture of free and  $\text{Mg}^{2+}$ -bound forms [39].

The effects of the adenine nucleotides vary in different CBS domain proteins. With the exception of the chloride channel CIC-1, which is inhibited by both AMP and ATP, generally AMP and ATP have opposite effects on these proteins [20]. For example, AMP activates and ATP inhibits AMP-activated protein kinase and the chloride channel CIC-2 [16,19], and, as in the case of *mtCBS*-PPase, ATP activates and AMP inhibits IMP dehydrogenase-2 and the chloride channel CIC-5. These findings have led to the hypothesis that CBS domains act as energy sensing modules in proteins [16]. Generally, AMP, ADP and ATP bind with similar affinities to these proteins, in contrast to adenine nucleotide interactions with *mtCBS*-PPase, where ADP binding is strongly preferred. Furthermore, AMP and ATP bind at least 100-fold, and ADP 10,000-fold, more tightly (in terms of  $K_d$ ) to *mtCBS*-PPase than to CIC-5 [29], or to other CBS domain proteins [16].

### Distribution, phylogeny, and possible role of CBS-PPases

Common type family II PPases predominate in *Bacilli*, whereas CBS-PPases predominate in *Clostridia* and sulfate-reducing delta-proteobacteria (supplementary material online, Figure S1). Both types of family II PPases occur sporadically in other bacterial lineages. In contrast, structurally distinct family I PPases are more widespread and occur in most of the eubacterial phyla as well as in archaea and eukaryotes. Interestingly, a majority of the CBS-PPases contain an ~120-amino acid DRTGG domain [40] between two CBS domains. The function of DRTGG domains is unknown, and they are found exclusively in bacterial and archaeal proteins. CBS-PPases from *M. thermoacetica* and *Syntrophomonas wolfei* are unique in that they possess CBS domains but lack a DRTGG domain.

Phylogenetic analysis of family II PPases suggests that all CBS-PPases are closely related but do not form a monophyletic group (supplementary material online, Figure S1). Some groups of common family II PPases, notably Bacilli PPases, have probably arisen due to the secondary loss of the CBS and DRTGG domain insertion. In addition, *M. thermoacetica* and *S. wolfei* are two independent cases where the DRTGG domain appears to have been lost. Finally, the clustering of CBS-PPases near the center of the tree suggests that the insertion was acquired very early in the evolution of family II PPases.

CBS-PPases are found in 16 of the 329 prokaryotic species with complete genomes sequences in the Kyoto Encyclopedia of Genes and Genomes ([www.genome.jp/kegg/catalog/org\\_list.html](http://www.genome.jp/kegg/catalog/org_list.html)). Thirteen of these 16 species also have a gene encoding a membrane-bound  $H^+$ -translocating PPase ( $H^+$ -PPase). Interestingly, none of the 83 prokaryotic species with a gene for  $H^+$ -PPase has a gene for the common family II PPase.  $H^+$ -PPase may be unnecessary when there is family II PPases because the latter are three orders

of magnitude more active and would therefore deplete the cell of  $PP_i$ , which  $H^+$ -PPase uses to establish a transmembrane pH gradient. In contrast, the activities of CBS-PPase and membrane-bound-PPase in *M. thermoacetica* are similar (A. Malinen, unpublished work), permitting control of the  $PP_i$  concentration by the levels of adenine nucleotides via *mtCBS*-PPase.

Biosynthetic reactions are the major source of  $PP_i$ . Accordingly, in *M. thermoacetica*, the intracellular level of  $PP_i$  peaks sharply during the mid-log phase of growth [41]. To avoid inhibition of biosynthetic enzymes and to provide  $P_i$  for ATP synthesis, this  $PP_i$  must be efficiently degraded by PPase. In fact, during the mid-log phase, *mtCBS*-PPase is expected to be most active because of a high  $[ATP]/([ADP] + [AMP])$  ratio. Interestingly,  $Co^{2+}$ , the best cofactor for *mtCBS*-PPase, is required for the growth of *M. thermoacetica* [22,42]. Metabolic stresses that decrease ATP production inhibit biosynthetic reactions and cell growth by decreasing the  $[ATP]/([ADP] + [AMP])$  ratio. This, in turn, should inhibit *mtCBS*-PPase and allow accumulation of  $PP_i$ , which would further inhibit biosynthetic reactions. Instead of or in conjunction with the action of  $H^+$ -ATPase, the accumulated  $PP_i$  is apparently used by  $H^+$ -PPase to sustain the pH gradient across the cell membrane and therefore maintain cell vitality. This two-PPase system may allow the cell to combat stress more efficiently than cells with only soluble or membrane-bound PPases. Thus, CBS-PPase may act as a survival factor under conditions of low energy supply.

In summary, unlike other PPases, *mtCBS*-PPase is subject to strong inhibition by AMP and ADP as well as activation by ATP. Remarkably, this enzyme binds adenine nucleotides much tighter than other reported CBS proteins. Furthermore, an effect of ADP, which is the most efficient inhibitor of *mtCBS*-PPase, is uncommon in other CBS proteins. Further studies, including determination of the three-dimensional structure of *mtCBS*-PPase with a bound adenine nucleotide, are needed to elucidate the structural basis for nucleotide regulation of this interesting enzyme and other CBS proteins.

This work was supported by Academy of Finland Grants 201611 and 114706, a grant for the National Graduate School in Informational and Structural Biology from the Ministry of Education and the Academy of Finland, and Russian Foundation for Basic Research Grant 06-04-48887. We thank P. V. Kalmykov for his assistance with analytical centrifugation.

## REFERENCES

- 1 Kornberg, A. (1962) On the metabolic significance of phosphorolytic and pyrophosphorolytic reactions. In Horizons in Biochemistry (Kasha, M. and Pullman, B., eds), pp. 251-264, Academic Press, New York
- 2 Heinonen, J. (2001) Biological Role of Inorganic Pyrophosphate, Kluwer Academic Publishers, Boston
- 3 Chen, J., Brevet, A., Formant, M., Leveque, F., Schmitter, J.-M., Blanquet, S. and Plateau, P. (1990) Pyrophosphatase is essential for growth of *Escherichia coli*. J. Bacteriol. **172**, 5686-5689
- 4 Lundin, M., Baltscheffsky, H. and Ronne, H. (1991) Yeast *PPA2* gene encodes a mitochondrial inorganic pyrophosphatase that is essential for mitochondrial function. J. Biol. Chem. **266**, 12168-12172
- 5 Sonnewald, U. (1992) Expression of *E. coli* inorganic pyrophosphatase in transgenic plants alters photoassimilate partitioning. Plant J. **2**, 571-581
- 6 Ogasawara, N. (2000) Systematic function analysis of *Bacillus subtilis* genes. Res. Microbiol. **151**, 129-134
- 7 Shintani, T., Uchiumi, T., Yonezawa, T., Salminen, A., Baykov, A. A., Lahti, R. and Hachimori, A. (1998) Cloning and expression of a unique inorganic pyrophosphatase from *Bacillus subtilis*. Evidence for a new family of soluble inorganic pyrophosphatases. FEBS Lett. **439**, 263-266
- 8 Young, T. W., Kuhn, N. J., Wadeson, A., Ward, S., Burges, D. and Cooke, G. D. (1998) *Bacillus subtilis* ORF *yybQ* encodes a manganese-dependent inorganic pyrophosphatase with distinctive properties: the first of a new class of soluble pyrophosphatase? Microbiology **144**, 2563-2571
- 9 Cooperman, B. S., Baykov, A. A. and Lahti, R. (1992) Evolutionary conservation of the active site of soluble inorganic pyrophosphatase. Trends Biochem. Sci. **17**, 262-266
- 10 Baykov, A. A., Cooperman, B. S., Goldman, A. and Lahti, R. (1999) Cytoplasmic inorganic pyrophosphatases. Progr. Mol. Subcell. Biol. **23**, 127-150
- 11 Aravind, L. and Koonin, E. V. (1998) A novel family of predicted phosphoesterases includes *Drosophila* prune protein and bacterial RecJ exonuclease. Trends Biochem. Sci. **23**, 17-19
- 12 Merckel, M. C., Fabrichniy, I. P., Salminen, A., Kalkkinen, N., Baykov, A. A., Lahti, R. and Goldman A (2001) Crystal structure of *Streptococcus mutans* pyrophosphatase: a new fold for an old mechanism. Structure **9**, 289-297

- 13 Ahn, S., Milner, A. J., Fütterer, K., Konopka, M., Ilias, M., Young, T. W. and White, S. A. (2001) The “open” and “closed” structures of the type-C inorganic pyrophosphatases from *Bacillus subtilis* and *Streptococcus gordonii*. *J. Mol. Biol.* **313**, 797-811
- 14 Parfenyev, A. N., Salminen, A., Halonen, P., Hachimori, A., Baykov, A. A. and Lahti, R. (2001) Quaternary structure and metal-ion requirement of family II pyrophosphatases from *Bacillus subtilis*, *Streptococcus gordonii* and *Streptococcus mutans*. *J. Biol. Chem.* **276**, 24511-24518
- 15 Bateman, A. (1997) The structure of a domain common to archaeobacteria and the homocystinuria disease protein. *Trends Biochem. Sci.* **22**, 12–13
- 16 Scott, J. W., Hawley, S. A., Green, K. A., Anis, M., Stewart, G., Scullion, G. A., Norman, D. G. and Hardie, D. G. (2004) CBS domains form energy-sensing modules whose binding of adenosine ligands is disrupted by disease mutations. *J. Clin. Invest.* **113**, 274–284
- 17 Ignoul, S. and Eggermont, J. (2005) CBS domains: structure, function, and pathology in human proteins. *Am. J. Physiol. Cell Physiol.* **289**, C1369–1378
- 18 Kemp, B. E. (2004) Bateman domains and adenosine derivatives form a binding contract. *J. Clin. Invest.* **113**, 182–184
- 19 Niemeyer, M. I., Yusef, Y. R., Cornejo, I., Flores, C. A., Sepúlveda, F. V. and Cid, L. P. (2004) Functional evaluation of human ClC-2 chloride channel mutations associated with idiopathic generalized epilepsies. *Physiol. Genomics* **19**, 74–83
- 20 Bennetts, B., Rychkov, G. Y., Ng, H.-L., Morton, C. J., Stapleton, D., Parker, M. W. and Cromer, B. A. (2005) Cytoplasmic ATP-sensing domains regulate gating of skeletal muscle ClC-1 chloride channels. *J. Biol. Chem.* **280**, 32452–32458
- 21 Wellhauser, L., Kuo, H.-H., Stratford, F. L. L., Ramjeesingh, M., Huan, L.-J., Luong, W., Li, C., Deber, C. M. and Bear, C. E. (2006) Nucleotides bind to the C-terminus of ClC-5. *Biochem. J.* **398**, 289–294
- 22 Drake, H. L. and Daniel, S. L. (2004) Physiology of the thermophilic acetogen *Moorella thermoacetica*. *Res. Microbiol.* **155**, 869–883
- 23 Sambrook, J. and Russel, D. W. (2001) *Molecular Cloning: A Laboratory Manual*. 3<sup>rd</sup> Ed., Cold Spring Harbor Laboratory Press, Cold Spring Harbor, New York
- 24 Gasteiger, E., Hoogland, C., Gattiker, A., Duvaud, S., Wilkins, M. R., Appel, R. D. and Bairoch, A. (2005) Protein identification and analysis tools on the ExPASy server. In *The Proteomics Protocols Handbook* (Walker, J. M., ed.), pp. 571-607, Humana Press Inc., Totowa



- 25 Baykov, A. A. and Avaeva, S. M. (1981) A simple and sensitive apparatus for continuous monitoring of orthophosphate in the presence of acid-labile compounds. *Anal. Biochem.* **116**, 1-4
- 26 Chervenka, C. H. (1972) *Methods for the Analytical Ultracentrifuge*. pp. 23–33, Spinco Division of Beckman Instruments, Inc., Palo Alto, CA
- 27 Baykov, A. A., Dudarenkov, V. Y., Käpylä, J., Salminen, T., Hyytiä, T., Kasho, V. N., Husgafvel, S., Cooperman, B. S., Goldman, A. and Lahti, R. (1995) Dissociation of hexameric *Escherichia coli* inorganic pyrophosphatase into trimers on His136 → Gln or His140 → Gln substitution and its effect on enzyme catalytic properties. *J. Biol. Chem.* **270**, 30804-30812
- 28 Kuhn, N. J., Wadeson, A., Ward, S. and Young, T. W. (2000) *Methanococcus jannaschii* ORF mj0608 codes for a class C inorganic pyrophosphatase protected by  $\text{Co}^{2+}$  or  $\text{Mn}^{2+}$  ions against fluoride inhibition. *Arch. Biochem. Biophys.* **379**, 292–298
- 29 Meyer, S., Savaresi, S., Forster, I. C. and Dutzler, R. (2007) Nucleotide recognition by the cytoplasmic domain of the human chloride transporter CLC-5. *Nature Str. Mol. Biol.* **14**, 60–66
- 30 Zyryanov, A. B., Vener, A. V., Salminen, A., Goldman, A., Lahti, R. and Baykov, A. A. (2004) Rates of elementary catalytic steps for different metal forms of the family II pyrophosphatase from *Streptococcus gordonii*. *Biochemistry* **43**, 1065–1074
- 31 Kery, V., Poneleit, L. and Kraus, J. P. (1998) Trypsin cleavage of cystathionine- $\beta$ -synthase into an evolutionarily conserved active core: structural and functional consequences. *Arch. Biochem. Biophys.* **355**, 222–232
- 32 Jhee, K. H., McPhie, P. and Miles, E. W. (2000) Domain architecture of the heme-independent yeast cystathionine- $\beta$ -synthase provides insights into mechanisms of catalysis and regulation. *Biochemistry* **39**, 10548–10556
- 33 Carr, G., Simmons, N. and Sayer, J. (2003) A role for CBS domain 2 in trafficking of chloride channel CLC-5. *Biochem. Biophys. Res. Comm.* **310**, 600–605
- 34 Bieman-Oldehinkel, E., Mahmood, N. B. N. and Poolman, B. (2006) A sensor for intracellular ionic strength. *Proc. Natl Acad. Sci. USA* **103**, 10624–10629
- 35 Zyryanov, A. B., Shestakov, A. S., Lahti, R. and Baykov, A. A. (2002) Mechanism by which metal cofactors control substrate specificity in pyrophosphatase. *Biochem. J.* **367**, 901–906
- 36 Zhang, R., Evans, G., Rotella, F. J., Westbrook, E. M., Beno, D., Huberman, E., Joachimiak, A. and Collart, F. R. (1999) Characteristics and crystal structure of bacterial inosine-5'-monophosphate dehydrogenase. *Biochemistry* **38**, 4691–4700

- 37 Miller, M. D., Schwarzenbacher, R., von Delft, F., Abdubek, P., Ambing, E., Biorac, T., Brinen, L. S., Canaves, J. M., Cambell, J., Chiu, H. J., Dai, X., Deacon, A. M., DiDonato, M., Elsliger, M. A., Eshagi, S., Floyd, R., Godzik, A., Grittini, C., Grzechnik, S. K., Hampton, E., Jaroszewski, L., Karlak, C., Klock, H. E., Koesema, E., Kovarik, J. S., Kreuzsch, A., Kuhn, P., Lesley, S. A., Levin, I., McMullan, D., McPhillips, T. M., Morse, A., Moy, K., Ouyang, J., Page, R., Quijano, K., Robb, A., Spraggon, G., Stevens, R. C., van den Bedem, H., Velasquez, J., Vincent, J., Wang, X., West, B., Wolf, G., Xu, Q., Hodgson, K. O., Wooley, J. and Wilson, I. A. (2004) Crystal structure of a tandem cystathionine-beta-synthase (CBS) domain protein (TM0935) from *Thermotoga maritima* at 1.87 Å resolution. *Proteins* **57**, 213–217
- 38 Dutzler, R., and Meyer, S. (2006) Crystal structure of the cytoplasmic domain of the chloride channel ClC-0. *Structure* **14**, 299–307
- 39 Phillips, R. (1966) Adenosine and the adenine nucleotides. Ionization, metal complex formation and conformation in solution. *Chem. Rev.* **66**, 501–527
- 40 Bateman, A., Coin, L., Durbin, R., Finn, R. D., Hollich, V., Griffiths-Jones, S., Khanna, A., Marshall, M., Moxon, S., Sonnhammer, E. L., Studholme, D. J., Yeats, C. and Eddy, S. R. (2004) The Pfam protein families database. *Nucleic Acids Res.* **32**, D138–141
- 41 Heinonen, J. and Drake, H. L. (1988) Comparative assessment of inorganic pyrophosphate and pyrophosphatase levels in *Escherichia coli*, *Clostridium pasterianum* and *Clostridium thermoaceticum*. *FEMS Microbiol. Lett.* **52**, 205–208
- 42 Lundie, L. L. and Drake, H. L. (1984) Development of a minimally defined medium for the acetogen *Clostridium thermoaceticum*. *J. Bacteriol.* **159**, 700–703

**Table 1 Effects of nucleotides and nucleosides (100  $\mu$ M) on  $\text{Co}^{2+}/\text{Mg}^{2+}$ -activated *mtCBS*-PPase**

The activity of *mtCBS*-PPase measured with no effector added ( $1.64 \text{ s}^{-1}$ ) was taken as 100%.

Effector	Activity (%)
None	100
Adenosine	$94 \pm 2$
AMP	$4.0 \pm 0.1$
ADP	< 1
ATP	$158 \pm 2$
cAMP	$42 \pm 4$
CDP	$50 \pm 8$
GMP	$82 \pm 3$
GDP	$81 \pm 3$
UDP	$65 \pm 8$
UTP	$96 \pm 2$
Cytidine, guanosine, uridine, CMP, CTP, GTP, cGMP, UMP	$100 \pm 3$

**Table 2 Parameters describing the effects of nucleotides on Co<sup>2+</sup>- and Mn<sup>2+</sup>-bound *mt*CBS-PPase**

Enzyme	Nucleotide	Co <sup>2+</sup> /Mg <sup>2+</sup> -activated enzyme		Mn <sup>2+</sup> /Mg <sup>2+</sup> -activated enzyme		Source
		A <sub>+L</sub> /A <sub>-L</sub> (%)	K <sub>d</sub> (μM)	A <sub>+L</sub> /A <sub>-L</sub> (%)	K <sub>d</sub> (μM)	
Wild type	AMP	3.7 ± 0.4	0.22 ± 0.02	20 ± 4	1.4 ± 0.2	Inhibition of activity (Figure 1)
	AMP		0.17 ± 0.05			Effect on AMP activation
	ADP	0.8 ± 0.3	0.012 ± 0.001	21 ± 2	0.033 ± 0.004	Inhibition of activity (Figure 1)
	ADP		0.017 ± 0.005			Effect on ADP activation (Figure 3)
	ATP	180 ± 10	0.20 ± 0.05	400 ± 40	7.2 ± 0.8	Inhibition of activity (Figure 1)
	ATP		0.16 ± 0.01			Effect on AMP inhibition
	ATP		0.6 ± 0.2			Effect on ADP inhibition (Figure 3)
	CDP	< 10	150 ± 20			Inhibition of activity
	UDP	< 10	340 ± 90			Inhibition of activity
Y169A	AMP	52 ± 2	5.3 ± 0.9			Inhibition of activity
	ADP	6.7 ± 0.4	0.21 ± 0.02			Inhibition of activity
	ATP	143 ± 4	2.4 ± 0.9			Inhibition of activity

## FIGURE LEGENDS

### Figure 1 Effects of adenine nucleotides on $\text{Co}^{2+}/\text{Mg}^{2+}$ -activated *mtCBS-PPase*

The *lines* show the best fit to eqn 1.

### Figure 2 Lineweaver-Burk plots for *mtCBS-PPase* inhibition and activation by adenine nucleotides

*Top panel*, Inhibition by AMP and activation by ATP. Numbers on the lines indicate AMP concentrations (in  $\mu\text{M}$ ). The line marked with *ATP* shows the effect of 10  $\mu\text{M}$  ATP. *Bottom panel*, Inhibition by ADP. Numbers on the lines indicate ADP concentrations (in  $\mu\text{M}$ ). The *insets* show the dependencies of  $K_{\text{m,app}}$  (*top panel*) or  $1/k_{\text{cat,app}}$  and  $k_{\text{cat,app}}/K_{\text{m,app}}$  (*bottom panel*) on nucleotide concentration.

### Figure 3 Combined effects of ADP and ATP on the activity of *mtCBS-PPase*

*Top panel*, Effect of various concentrations of ADP at several fixed concentrations of ATP. *Bottom panel*, Effect of various concentrations of ATP at several fixed concentrations of ADP. The numbers on the curves denote the fixed concentration of the second nucleotide in  $\mu\text{M}$ . The *lines* show the best fit to eqn 1. The *insets* show the dependences of  $K_{\text{d,app}}$  value on the concentration of the corresponding fixed ligand. The *lines* in the *insets* show the best fit to eqn 2.

### Figure 4 SDS-PAGE analysis of *mtCBS-PPase*

Lane *a*, molecular mass markers; lane *b*, intact enzyme; lane *c*, enzyme crosslinked with glutaraldehyde for 15 min; lane *d*, enzyme crosslinked with glutaraldehyde for 30 min. Protein load for lanes *b–d* was 1  $\mu\text{g}$  per lane.

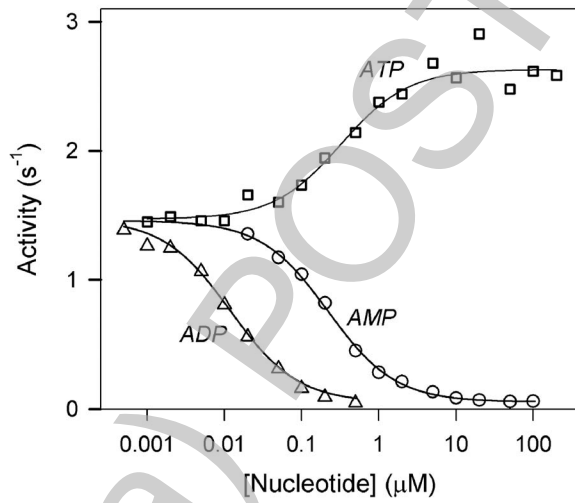


Figure 1

Stage 2 (a) POST-PRINT

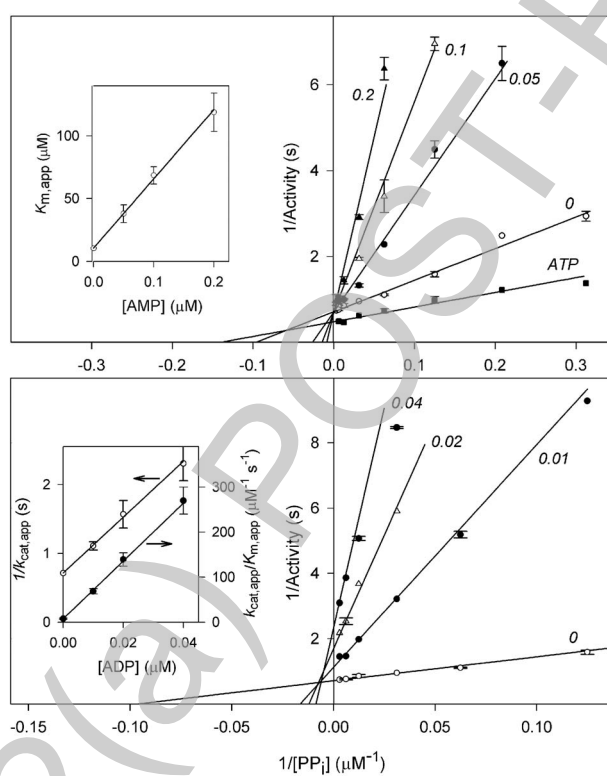


Figure 2

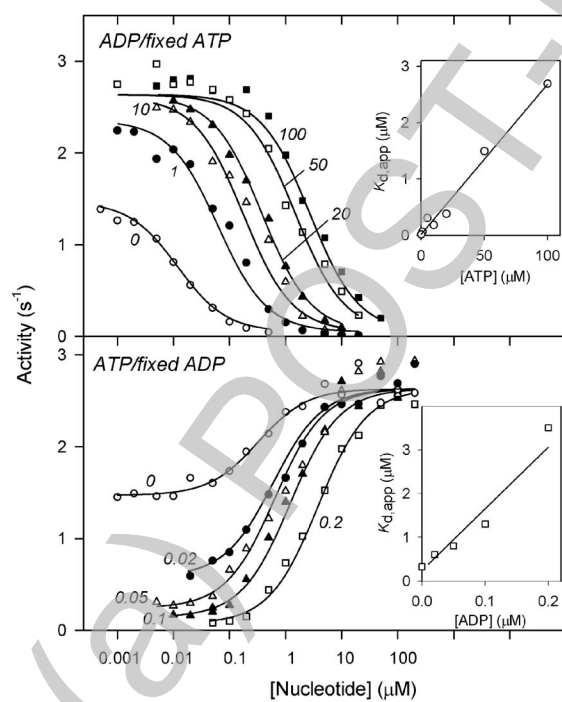


Figure 3



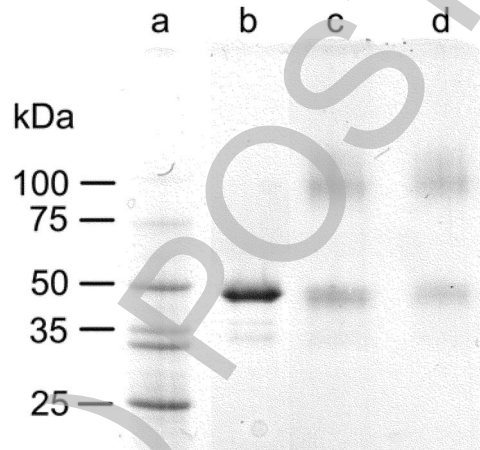


Figure 4